

MARS' OBLIQUITY-DRIVEN MOBILE CO₂ INVENTORY DERIVED FROM POLAR STRATIGRAPHY.

P. B. Buhler^{1,2}, S. Piqueux¹. ¹Jet Propulsion Laboratory, California Institute of Technology. Now at Planetary Science Institute (pbuhler@psi.edu).

Introduction: CO₂ adsorbed in the martian regolith was detected over 40 years ago by Viking Lander 1 [1]. Subsequent studies suggested that the adsorbed CO₂ reservoir may be significantly larger than the combined mass of Mars' 96% CO₂ atmosphere and South Polar Massive CO₂ Ice Deposit (MCID) and, if true, that the process of CO₂ adsorption in the martian regolith could significantly affect Mars' pressure—and therefore climate—evolution over obliquity cycles [2]. Nevertheless, due to its poorly known mass and spatial extent, the adsorbed CO₂ reservoir is often ignored in martian climate investigations [3]. However, because the evolution of Mars' atmosphere, regolith, and MCID are intimately coupled, the climate record stored in the stratigraphy of the MCID provides a record of how these three exchangeable CO₂ reservoirs co-evolve. We use a numerical climate model of MCID stratigraphic evolution as a function of Mars' orbital evolution [4] to determine the mass of the mobile CO₂ inventory participating in exchange between the regolith, MCID, and atmospheric CO₂ reservoirs over obliquity cycles (Fig. 1).

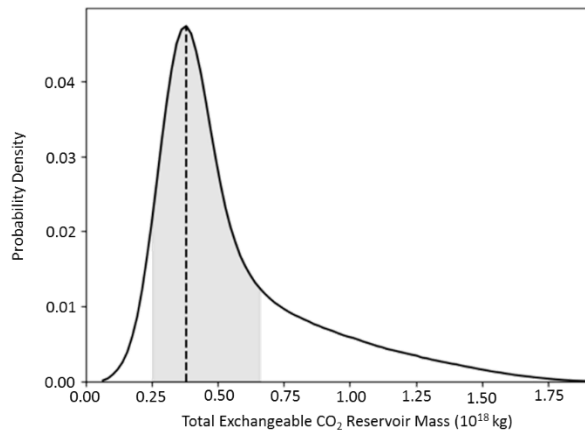


Fig. 1: Model-derived probability distribution for mobile CO₂ inventory participating in exchange between regolith, MCID, and atmospheric CO₂ reservoirs over obliquity cycles.

Methods: We adopt a framework in which changes to Mars' mean annual latitudinal insolation, due to Mars' orbital evolution, thermodynamically drive the exchange of CO₂ between the atmosphere, MCID, and regolith. Atmospheric CO₂ is in contact with both the regolith and the MCID, while the MCID and regolith exchange CO₂ indirectly, through the atmosphere. CO₂ exchange between reservoirs is not kinetically hindered on timescales relevant to Mars' orbital variations [5,6].

Atmosphere-MCID CO₂ exchange is determined by polar energy balance and vapor pressure equilibrium, according to the methods in [5]:

$$(Eq. 1) \quad P_{eq,cap} = P_{eq,0} \exp \left[-\frac{z_{base} + \frac{m_{cap}}{A_{cap} \times \rho}}{H} \right]$$

Here $P_{eq,cap}$ is the equilibrium pressure at the elevation of the upper surface of the MCID, set by the MCID base elevation z_{base} plus the MCID thickness, which depends on CO₂ ice density ρ and MCID mass m_{cap} and area A_{cap} . $P_{eq,0}$ is pressure at the zero-elevation datum, which is also the mean elevation of the regolith surface.

The regolith is divided into a grid of latitude and depth. The mass of adsorbed CO₂ dm_{reg} in each box is calculated based upon $P_{eq,0}$ and temperature T as a function of depth z , using [7]:

$$(Eq. 2) \quad dm_{reg} = dV_{reg} A_S \delta P_{eq,0}^\gamma T(z)^\beta$$

dV_{reg} is the regolith volume of a given grid box, A_S is the regolith specific surface area, and δ , γ , and β are values fit to empirical data [7]. The total mass of CO₂ adsorbed in the regolith m_{reg} is the integral over all the dm_{reg} elements. Temperature is calculated from a 1-dimensional energy balance model that accounts for incoming absorbed insolation energy flux, outgoing emitted thermal energy flux, and the energy flux conducted to the subsurface. Subsurface temperature is calculated using the diffusion equation [5] with a regolith heat capacity of 837 J kg⁻¹ K⁻¹, density of 2000 kg m⁻³ [2].

Mars' total exchangeable CO₂ is $m_{tot} = m_{atm} + m_{cap} + m_{reg}$, a conserved quantity in our model. We model how m_{tot} partitions between m_{atm} , m_{cap} , and m_{reg} for various obliquities ϵ . For each ϵ , we iteratively compute atmosphere-MCID and atmosphere-regolith equilibria until the mass of each reservoir is within 0.1% of the mass from the previous iteration (Fig. 1). We then construct the temporal evolution of the partitioning of Mars' CO₂ inventory by interpolating between ϵ grid points to find the mass of each reservoir for any desired ϵ (Fig. 2). Eccentricity and longitude of perihelion are set to 0 because the distribution of CO₂ ice is more sensitivity to ϵ than other orbital parameters [3,5].

The MCID stratigraphy of alternating CO₂ and H₂O ice layers evolves as H₂O ice in the CO₂ consolidates into lag layers when CO₂ ice ablates and older ice layers are buried when of CO₂ ice accumulates [5].

We then run the climate model over a range of regolith albedo (0.2 - 0.3) [3], thermal conductivity (0.08 - 2.0 W m⁻¹ K⁻¹), regolith specific surface area (10² - 10⁵ m² kg⁻¹) [7,9], and regolith thickness (1 m - 1 km) [2,7]. For each parameter set, we obtain a model-derived stratigraphy. This work focuses on how varying regolith

parameters affects MCID stratigraphy, so we do not explore the effect of varying model parameters relating to the polar CO₂ ice, but rather adopt values from [5]. We also do not vary regolith emissivity (set to 1.0) or the geothermal gradient (0.03 W m^{-2} [10]), because these parameters are degenerate with albedo and thermal conductivity, respectively.

Finally, we perform Markov Chain Monte Carlo analysis to compare the model-derived stratigraphy for a particular parameter set to observations in order to determine the likelihood of the mass of the mobile CO₂ inventory participating in exchange between the regolith, MCID, and atmospheric CO₂ reservoirs over obliquity cycles (Fig. 1). We use observed volume fractions of the CO₂ layers in the MCID of: top, 77%; middle, 21%; bottom, 2% [8,11, I.B. Smith per. comm.].

Results: Models in which the total accessible mobile inventory of CO₂ on obliquity timescales is 100^{+80}_{-34} mbar ($3.8^{+3.0}_{-1.3} \times 10^{17} \text{ kg}$) yield stratigraphies that are most consistent with the observed MCID stratigraphy (Fig. 1).

In general, larger CO₂ inventories lead to larger top layers and smaller bottom layers, and vice versa. This is because, when regolith adsorptive capacity is larger, the variation in MCID mass extrema are larger, meaning that proportionally less CO₂ survives obliquity maxima. Likewise, the upper layers are thicker because more CO₂ fluxes back onto the cap during the recent lower obliquity periods. CO₂ mass in the atmosphere, cap, and regolith are shown as a function of obliquity in Fig. 2.

Discussion and Conclusions: Previous attempts to model Mars' exchangeable CO₂ inventory on obliquity cycles [2,7] did not have the benefit of comparison to the record of CO₂ exchange stored in the MCID stratigraphy. Instead, they relied on the best observations of the time, which indicated that Mars had an insignificant polar CO₂ ice deposit. As a result, the task of identifying Mars' total CO₂ inventory was under-constrained and required previous investigators to select their preferred value of regolith adsorptive capacity. Fortunately, the MCID provides a geologic record of CO₂ exchange between the atmosphere, MCID, and regolith [5,8]. The modern observations of the MCID available to our study (the ratio of multiple MCID layers rather than the binary presence/absence of a polar CO₂ ice deposit) sufficiently constrain statistical determination of the best-fit parameters, eliminating the need to select regolith adsorptive capacity as a model input.

The best-fit exchangeable CO₂ inventory on obliquity cycles determined in our model is intermediate between previous estimates: 30-40 mbar [7] and 65-514 mbar [2].

Acknowledgments: Part of this work was performed at the Jet Propulsion Laboratory, California Institute of Technology,

under a contract with NASA. © 2020, All Rights Reserved.

References: [1] Oyama, V.I. et al. (1977) *JGR* 82, 4669-76; [2] Fanale, F.P. et al. (1982) *Icarus* 50, 381-407; Haberle et al., 2003; [3] Haberle, R.M. et al. (2003) *PSS* 56, 251-255; [4] Laskar, J. et al. (2004) *Icarus* 170, 343-364; [5] Buhler, P.B et al. (2020) *Nat. Astron.* 4(4), 364-371; [6] Schorghofer, N. and Forget, F. (2012) *Icarus* 220, 1112-1120; [7] Zent, A.P. & Quinn, R.C. (1995) *JGR* 100, 5341-49; [8] Bierson, C. et al. (2016) *GRL* 43, 4172-79; [9] Nielsen, M.E. & Fisk, M.R. (2010) *GRL* 37(15). [10] Dehant, V., et al. (2012) *PSS* 68, 123-145. [11] Alwarda, R. & Smith, I.B. (2019) *50th LPSC #2132*.

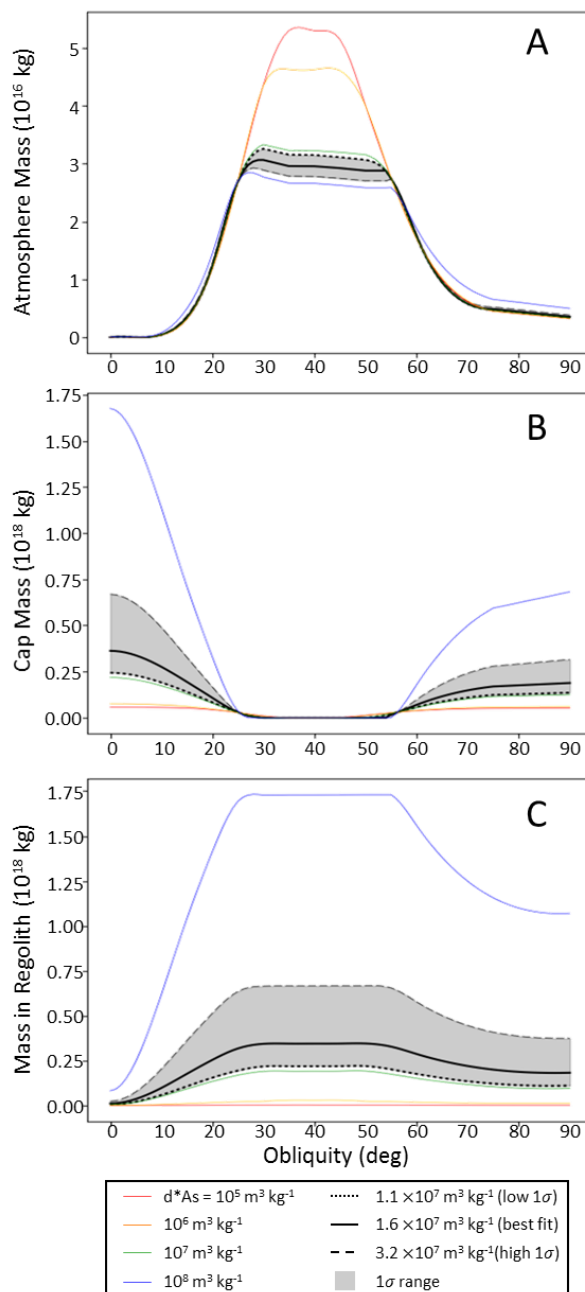


Fig. 2. The mass in each reservoir (A. Atmosphere, B. Cap, C. Regolith) as a function of obliquity for various values of regolith adsorptive potential (depth \times specific surface area).